

Role of computed tomography angiography in detection and staging of small bowel carcinoid tumors

David Bonekamp, Siva P Raman, Karen M Horton, Elliot K Fishman

David Bonekamp, Siva P Raman, Karen M Horton, Elliot K Fishman, the Russell H. Morgan Department of Radiology and Radiological Science, the Johns Hopkins Medical Institutions, Baltimore, MD 21287, United States

Author contributions: Bonekamp D and Fishman EK made the conception of study; Fishman EK acquired the data; Bonekamp D drafted up the manuscript; all the authors analyzed the imaging studies, revised the paper and made the final approval.

Conflict-of-interest statement: All the author have no conflict of interest.

Open-Access: This article is an open-access article which was selected by an in-house editor and fully peer-reviewed by external reviewers. It is distributed in accordance with the Creative Commons Attribution Non Commercial (CC BY-NC 4.0) license, which permits others to distribute, remix, adapt, build upon this work non-commercially, and license their derivative works on different terms, provided the original work is properly cited and the use is non-commercial. See: <http://creativecommons.org/licenses/by-nc/4.0/>

Correspondence to: Elliot K Fishman, MD, Professor, the Russell H. Morgan Department of Radiology and Radiological Science, the Johns Hopkins Medical Institutions, 601 N. Caroline Street, JHOC 3140C, Baltimore, MD 21287, United States. efishman@jhmi.edu
Telephone: +1-410-9555173
Fax: +1-410-6140341

Received: May 4, 2015
Peer-review started: May 5, 2015
First decision: June 3, 2015
Revised: June 18, 2015
Accepted: August 4, 2015
Article in press: August 7, 2015
Published online: September 28, 2015

Abstract

Small-bowel carcinoid tumors are the most common form (42%) of gastrointestinal carcinoids, which by

themselves comprise 70% of neuroendocrine tumors. Although primary small bowel neoplasms are overall rare (3%-6% of all gastrointestinal neoplasms), carcinoids still represent the second most common (20%-30%) primary small-bowel malignancy after small bowel adenocarcinoma. Their imaging evaluation is often challenging. State-of-the-art high-resolution multiphasic computed tomography together with advanced postprocessing methods provides an excellent tool for their depiction. The manifold interactive parameter choices however require knowledge of when to use which technique. Here, we discuss the imaging appearance and evaluation of duodenal, jejunal and ileal carcinoid tumors, including the imaging features of the primary tumor, locoregional mesenteric nodal metastases, and distant metastatic disease. A protocol for optimal lesion detection is presented, including the use of computed tomography enterography, volume acquisition, computed tomography angiography and three-dimensional mapping. Imaging findings are illustrated with a series of challenging cases which illustrate the spectrum of possible disease in the small bowel and mesentery, the range of possible appearances in the bowel itself on multiphase data and extraluminal findings such as the desmoplastic reaction in mesentery and hypervascular liver metastases. Typical imaging pitfalls and pearls are illustrated.

Key words: Small bowel carcinoid; Multidetector computed tomography; Multiplanar analysis; Volume rendered technique; Maximum intensity projection; Surface shading technique

© **The Author(s) 2015.** Published by Baishideng Publishing Group Inc. All rights reserved.

Core tip: Small-bowel carcinoid tumors are neuroendocrine tumors and represent most common form of gastrointestinal carcinoids. Although primary small bowel neoplasms are overall rare, carcinoids still represent the second most common primary small-bowel malignancy. State-of-the-art high-resolution multiphasic computed

tomography with advanced postprocessing methods provides an excellent tool to overcome the challenges of their depiction. Here, we discuss their imaging appearance, focusing on the primary tumor, locoregional mesenteric nodal metastases, and distant metastatic disease. Guidance for imaging protocol selection is given. Imaging findings are illustrated with a series of challenging cases which illustrate the spectrum of disease. Typical imaging pitfalls and pearls are illustrated.

Bonekamp D, Raman SP, Horton KM, Fishman EK. Role of computed tomography angiography in detection and staging of small bowel carcinoid tumors. *World J Radiol* 2015; 7(9): 220-235 Available from: URL: <http://www.wjgnet.com/1949-8470/full/v7/i9/220.htm> DOI: <http://dx.doi.org/10.4329/wjrr.v7.i9.220>

INTRODUCTION

Small-bowel carcinoid tumors are classically defined as histologically well-defined neuroendocrine tumors (NET). NET arise from cells of the diffuse neuroendocrine system and occur primarily in the form of gastrointestinal carcinoid (GI-carcinoid) (70%)^[1,2], tracheobronchial carcinoid (25%)^[2,3] and pancreatic neuroendocrine tumors. GI-carcinoid and pancreatic neuroendocrine tumors are occasionally classified together into a group of gastroenteropancreatic tumors^[4]. Many other organs can be site of origin for NET, such as the kidney, gonads and gallbladder^[5,6]. Gastrointestinal carcinoids occur most commonly in the small bowel (42%), while 27% occur in the rectum and 9% in the stomach^[2]. Gastrointestinal carcinoids are multiple in up to 40% and associated with second primary malignancies in up to 50%. Gastrointestinal carcinoids are relatively uncommon and represent only about 2% of all gastrointestinal tumors^[7], with an incidence of 2 per 100000 worldwide annually^[8]. As primary small bowel neoplasms are overall rare (3%-6% of all gastrointestinal neoplasms), carcinoids still represent the second most common (20%-30%) primary small-bowel malignancy^[7,9,10] after small bowel adenocarcinoma^[9].

In this article, we discuss the imaging appearance and evaluation of duodenal, jejunal and ileal carcinoid tumors, including the imaging features of the primary tumor, locoregional mesenteric nodal metastases, and distant metastatic disease are discussed. In addition, a protocol for optimal lesion detection is presented, including the use of CT enterography, volume acquisition, CT angiography (CTA) and three-dimensional (3D) mapping. Imaging findings are illustrated with a series of challenging cases which nicely illustrate the spectrum of possible disease in the small bowel and mesentery, the range of possible appearances in the bowel itself on multiphase data and extraluminal findings such as the desmoplastic reaction in mesentery and hypervascular liver metastases. Typical imaging pitfalls and pearls are

illustrated.

SMALL BOWEL CARCINOID TUMORS, PATHOLOGY, CLINICAL PRESENTATION AND EPIDEMIOLOGY

Small bowel carcinoid tumors arise from as many as 14 different specialized endocrine cell types (*e.g.*, EC-cells, G-cells, D-cells, *etc.*) of the diffuse endocrine system that lines the gastrointestinal mucosa and submucosa^[11-14], and belong to the group of apudomas (amine precursor uptake and decarboxylation tumors). Most small bowel carcinoids arise from enterochromaffine (argentaffine) Kulchitsky's cells in the Lieberkuhn crypts which are most prevalent in the distal ileum and which produce serotonin^[15]. Forty percent of small bowel carcinoids are located within 60 cm of the ileocecal valve^[16]. These classic serotonin-producing small intestinal carcinoids are the most common form, and represent about 42% of gastrointestinal carcinoids^[3]. Once hormone production overwhelms the metabolic capacity of the liver, commonly after the development of liver metastases, the carcinoid syndrome ensues (observed in up to 20% of patients), which consists of diarrhea, bronchospasm, flushing, abdominal cramps and carcinoid heart disease^[17]. In some instances, small bowel carcinoid tumors may be found as an unusual cause of gastrointestinal bleeding^[18] or incidentally after resection of a Meckel's diverticulum^[19]. In rare instances a midgut carcinoid tumor may invade the retroperitoneal venous circulation and lead to the earlier development of carcinoid syndrome before liver metastases occur^[20]. Conversely, nonfunctioning carcinoids have a propensity to present with extensive liver metastases^[12]. The average age at diagnosis is 61-64 years^[2,12,21], and GI carcinoids are more common in males and African Americans, except for appendiceal and bronchopulmonary carcinoid tumors^[2,8]. The diagnosis is suggested by elevated plasma serotonin or chromogranin A levels and elevated urinary 5-hydroxyindoleacetic acid levels^[12]. Synchronous and metachronous malignancies occur in 30%^[2], most commonly gastrointestinal adenocarcinoma^[22], however the increased rates of other primary malignancies may reflect the relatively good prognosis of patients with this diagnosis compared to other GI cancers^[14]. Focal nodular, polypoid and infiltrative growth patterns of small bowel carcinoid tumors occur. An infiltrative growth pattern with associated desmoplastic reaction is typical, in which tumor cells insinuate between the muscularis propria. There, tumor cells locally release serotonin and other (including vasoactive) substances, which incite a dense fibrosis and desmoplasia. Vasoactive substances may cause strictures and caliber irregularities of local mesenteric vessels, which result in elastic vascular sclerosis. While overall less aggressive and slower growing than small-bowel adenocarcinoma, small bowel carcinoid tumors are not uncommonly

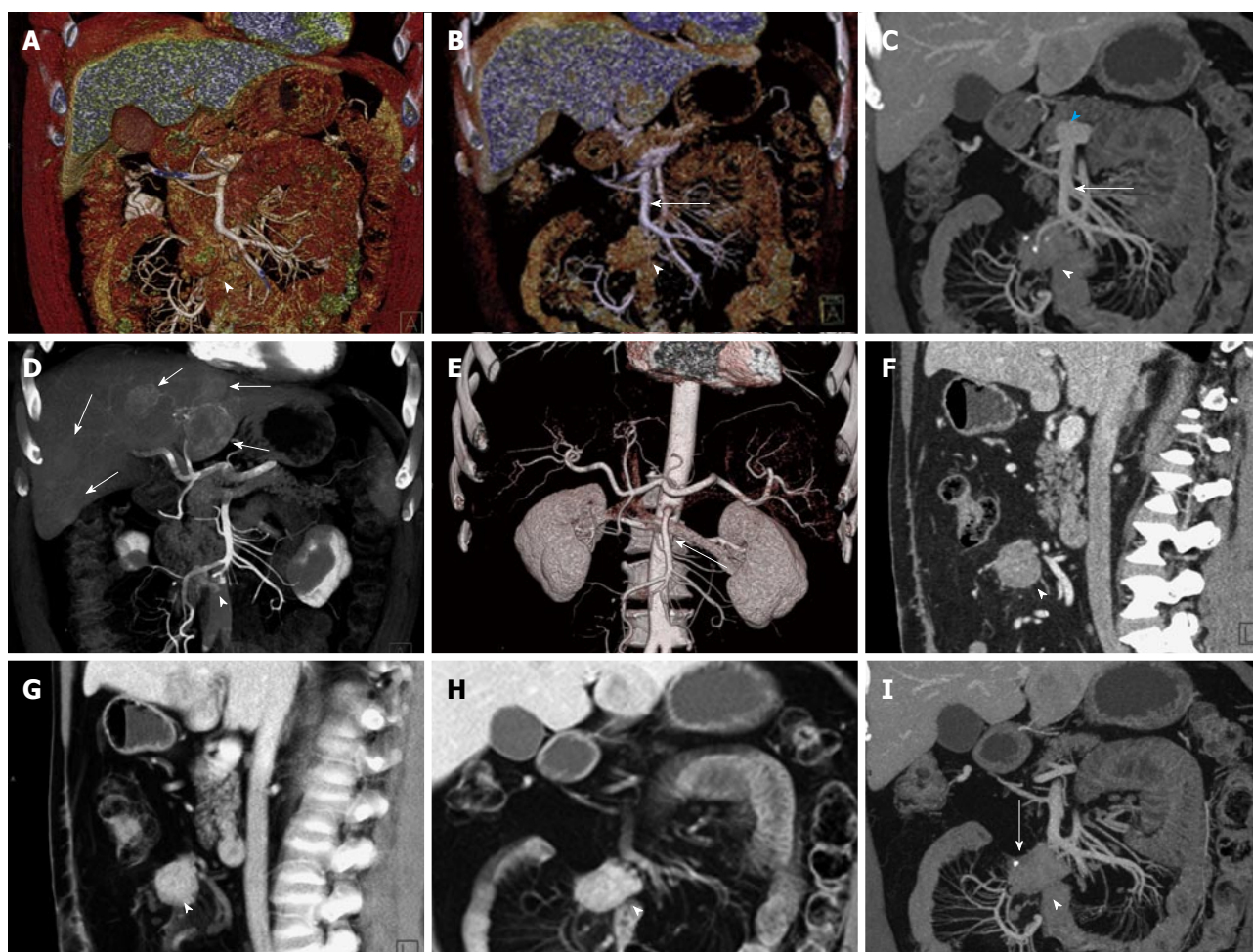


Figure 1 General use of maximum intensity projections, multiplanar reconstructions, volume rendered technique and surface shading. A, B: Coronal surface rendering technique with two different window settings allows to obtain a 3D understanding of a mesenteric mass (arrowhead) and its relationship to the SMV (arrow). The lower window setting (A) includes more soft tissue detail, and better depicts the mesenteric structures and adjacent bowel loops, while the higher window setting (B) excludes structures with lower attenuation and focuses the view on vascular morphology; C: Coronal venous phase VRT image showing the mesenteric mass with calcifications (arrowhead), and the relationship to the SMV (arrow), which can be visualized in its entire course to the portosplenic confluence (blue arrowhead); D: Volume rendering of arterial phase CTA data simultaneously depicts hypervascular liver metastases (arrows) and the relationship of the mesenteric mass to the SMA with vascular encasement and rarefaction of SMA branches (arrowhead); E: 3D surface shading has its major advantage in the depiction the vascular anatomy (SMA, arrow), while the chosen windowing reduces the conspicuity of the mesenteric mass (arrowhead) and removes the voxels pertaining to the liver metastases and the hepatic parenchyma for depiction of the hepatic arteries; F, G: Comparison of sagittal venous phase slice (F) and VRT postprocessed image (G). The mesenteric mass (arrowheads) and its relationship to the adjacent vessels is better defined with VRT (G); H, I: Comparison of coronal VRT (H) to coronal thick slab MPR (I). While VRT makes the spatial relationships more apparent, MPR better demonstrates vascular anatomical detail and the relationship of vessels to the mesenteric mass (arrowheads). Also, a small calcification in the mesenteric mass (arrow) is only visualized with MPR, while the VRT algorithm hides this important detail. VRT: Volume rendered technique; MPR: Multiplanar reconstructions; MIP: Maximum intensity projections; SMV: Superior mesenteric vein; CTA: Computed tomography angiography; SMA: Superior mesenteric artery; 3D: Three-dimensional.

diagnosed in advanced stages (metastatic disease is present in 43% and distant metastases in 13%-24% of patients at the time of diagnosis), such that the rate of metastatic disease approaches that of other GI cancers^[2,14]. The rate of metastatic disease depends on the size of the primary tumor: Nodal metastatic disease occurs in 20%-30% of tumors less than 1 cm in size and increases to more than 80% in tumors more than 2 cm in size. Liver metastases are observed in up to 20% if the primary tumor is less than 2 cm in size, and more than 40% if it is larger than 2 cm^[23-25]. Compared to all GI cancers, GI carcinoid has an overall favorable prognosis, with a relative survival rate of 87% (compared to 53% for GI cancers). GI carcinoid 5-year survival rates are 89% for regional and 59%

for distant stage disease, compared to 56% and 9% for all GI cancers^[14]. The main potentially curative therapy is surgical resection, as carcinoid tumors are often resistant to chemotherapy, although somatostatin analogs (*e.g.*, octreotide) can significantly prolong the time to disease progression in patients with functioning carcinoids^[26]. If tumor control by the use of surgery, chemotherapy or somatostatin therapy cannot be achieved, median patient survival is 30 mo, whereas patients with distant metastatic disease have a reduced median survival of 23 mo. In patients who died of the disease after a mean follow-up of 70 mo in a study of more than 25000 patients, the 5 year survival rate was 29%, underlining the aggressive potential of the disease in some patients^[14]. The median survival of treatment

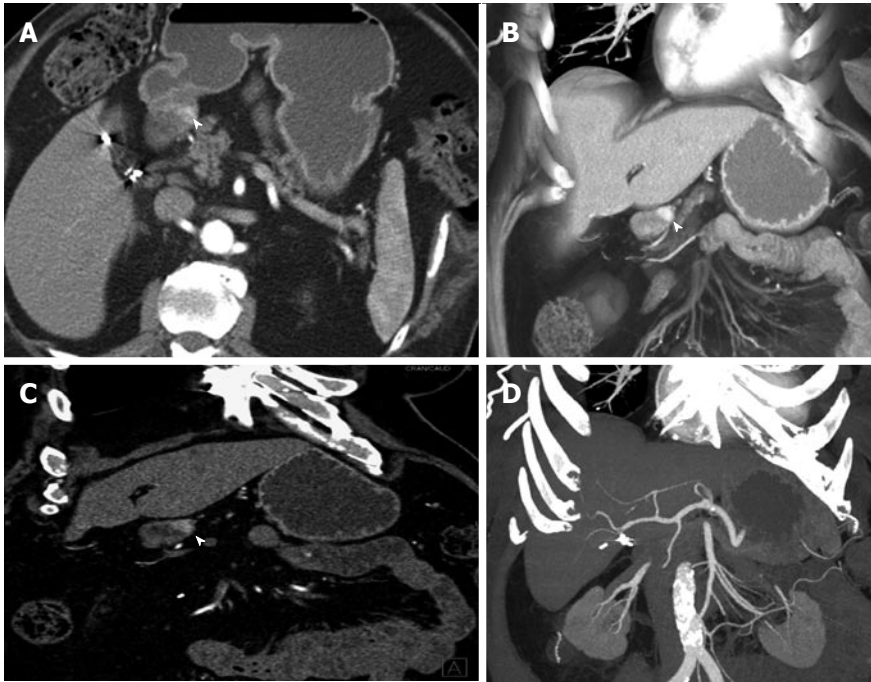


Figure 2 Duodenal carcinoid. A 80-year-old male with duodenal carcinoid. Upper endoscopy for screening showed 1.5 cm mass in the 1st portion of the duodenum. An attempt at endoscopic resection failed, as the mass was too deeply located and invaded the muscularis propria. This case well demonstrates the imaging appearance of the intramural primary tumor as hypervascular mass and the choice of 3D postprocessing methods for optimal evaluation. A: On axial arterial phase imaging, the mass in the wall of the 1st portion of the duodenum is quite subtle (arrowhead). The mass is much better depicted on a coronal VRT image (B) or a thin slab coronal MPR (C), improving diagnostic confidence, while coronal MIP (D) does not provide good contrast in this case. VRT: Volume rendered technique; MPR: Multiplanar reconstructions; 3D: Three-dimensional; MIP: Maximum intensity projections.

resistant GI carcinoids has not improved over time, and the overall mortality has increased, suggesting that the overall improved prognosis, which may be due to increased incidence (higher rates of incidental and early diagnosis), is not counterbalanced by improved therapeutic success in advanced stage or treatment resistant disease^[14].

A traditional belief has been that appendiceal carcinoids are the most common form of GI carcinoid^[27], with a distinctly higher 5 year survival rate approximating 99% for all stages compared to other gastrointestinal carcinoid tumors^[27]. Earlier studies were based on data from large epidemiological programs, where data recorded between 1950 and 1969 from the End Results Group (ERG) yielded a partition of appendiceal carcinoids of 44%, and data recorded between 1969 and 1971 from the Third National Cancer Survey (TNCS) of the National Cancer Institute (NCI) of 36%^[2,27]. More recent data extracted from the Surveillance, Epidemiology and End Results (SEER) program of the NCI between 1973 and 1999 showed a drastically different result, with appendiceal carcinoids representing only 2.4% of gastrointestinal carcinoids, with a pan-SEER incidence of 4.8%^[2]. A recent updated analysis of the SEER database between 1973 and 2009 showed an annual percent decrease of appendiceal carcinoid of 3.6%, suggesting a noticeable decrease over time. Advances in immunohistochemistry and histological analysis as well as differences in data reporting may be responsible for the observed discrepancies of the

reported numbers of appendiceal carcinoid tumors in the pre-SEER period. Further contributing factors may be the decreasing number of appendectomies performed, and better ability to differentiate carcinoid from inflammatory appendicitis on pathology^[2,14,28,29]. A large study by Modlin *et al.*^[2] reported data accumulated over 30 years, and suggested an overall increase of the incidence of carcinoid tumors over the past decades, and this finding has been supported by other studies^[8,14,30,31], including a recent update^[32]. Gastric and rectal carcinoids demonstrated a marked increase (up to approximately 4-fold). The increase of gastric carcinoids has been associated with the increased use of proton pump inhibitors^[33]. Rectal carcinoid, appendiceal carcinoid and gastric carcinoid are more commonly discovered incidentally, as these tumors are less often hormonally active and exhibit a more indolent clinical course, with the exception of the sporadic Type 3 gastric carcinoids.

Duodenal carcinoid

Although the duodenum can be considered the most proximal part of the small bowel, it is anatomically formed at the junction between foregut and midgut, while the jejunum and ileum are exclusively midgut derivatives. As a result, the cellular composition of duodenal carcinoid tumors and their syndromic association varies from other small bowel carcinoids. Duodenal carcinoid is rare, and accounts for only 2%-3% of all gastrointestinal neuroendocrine tumors^[2]. The majority

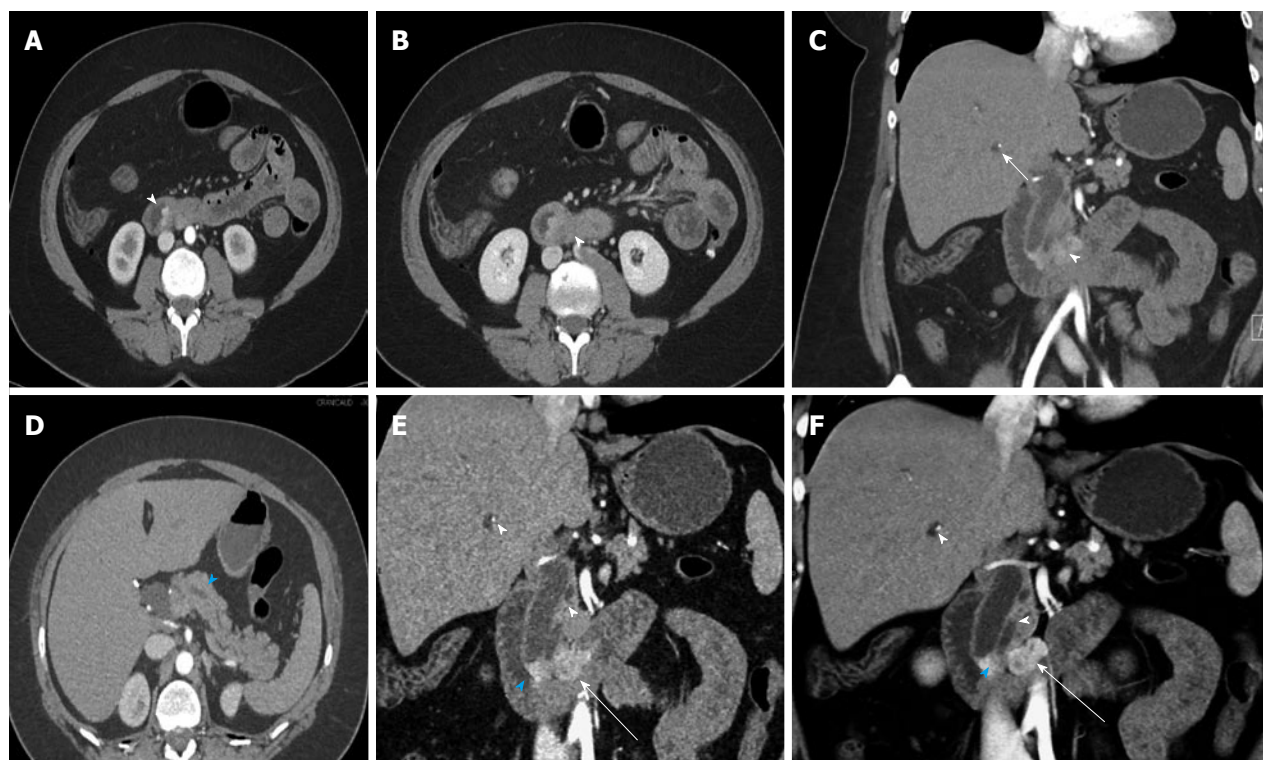


Figure 3 Ampullary neuroendocrine tumor. A 49-year-old female with 1.2 cm neuroendocrine neoplasm of the ampulla, metastatic to the liver. The tumor was incidentally found due to dilated biliary and pancreatic ducts on a renal protocol computed tomography (CT). The patient underwent classic pancreaticoduodenectomy and liver wedge resection, confirming a low grade (G1) 1.2 cm neuroendocrine neoplasm of the ampulla with invasion of the pancreas and peripancreatic tissues. 1 of 19 lymph nodes was involved and lymphovascular invasion was present. This case demonstrates the typical imaging appearance of a hypervascular intramural primary carcinoid, with additional specific imaging features of a periampullary mass. The case also illustrates important aspects of 3D postprocessing. Axial arterial phase (A) and venous phase (B) CT angiography (CTA) images of the 2nd portion of the duodenum show a hypervascular mass in the ampulla (arrowheads). C: Coronal arterial phase image shows the hypervascular mass extending outside the duodenal wall, with adjacent hypervascular peripancreatic lymph nodes (arrowhead). Intrahepatic biliary ductal dilation is noted (arrow); D: Pancreatic ductal dilation results from the obstructing ampullary mass (arrowhead); E, F: Thick slab MPR (E) and VRT (F) images better depict the spatial relationships: The ampullary mass (blue arrowheads) causes moderate extrahepatic and intrahepatic biliary ductal dilation (arrowheads). Peripancreatic hypervascular lymph node metastases (arrows) are present. Note the advantage of MPR and VRT over axial slices in making the mass much more apparent. VRT: Volume rendered technique; MPR: Multiplanar reconstructions; 3D: Three-dimensional.

of duodenal carcinoids are G-cell tumors (62%). A more rare form, D-cell carcinoids, produce somatostatin, and account for 21% of duodenal carcinoids. They occur exclusively around the ampulla of Vater and are strongly associated with neurofibromatosis type 1, with up to 50% of patients with D-cell duodenal carcinoid carrying a diagnosis of neurofibromatosis type 1. The periampullary location is associated with symptoms of ampullary obstruction, including obstructive pancreatitis and biliary obstruction with jaundice. On histology, psammoma bodies are typically found. Classic EC-cell serotonin producing carcinoids, which are most common in the midgut, are rare in the duodenum. Of all duodenal carcinoids, one third are functioning (hormonally active) carcinoids, typically G-cell tumors producing gastrin, resulting in the clinical manifestation of Zollinger-Ellison syndrome (ZES). G-cell tumors with elevated serum gastrin are termed gastrinomas. Duodenal carcinoids are associated with multiple endocrine neoplasia type 1 (MEN-1), and 90% of duodenal carcinoids occurring in MEN-1 are G-cell carcinoids. These MEN-1 duodenal carcinoids are typically multiple, with individual tumors measuring less 5 mm and showing a predilection for

the proximal duodenum. The mean age at diagnosis is 53 years, however the observed age range is wide, and tumors have been diagnosed in patients ranging from 19-90 years old. 85% of sporadic gastrinomas occur anatomically in the gastrinoma triangle, which is formed by the cystic duct/CBD junction superiorly, the inferior genu of the duodenum inferiorly and the junction of the neck and body of the pancreas medially. Not all of these tumors are technically small bowel carcinoids in the narrow sense if they primarily arise from the biliary ductal system or the pancreas, although there may not be a clear distinction as to the origin if the lesion is large. Duodenal carcinoids demonstrate an intraluminal polypoid growth in 50%, while an intramural growth pattern is found in 40%.

Jejunal and ileal carcinoids

Jejunal and ileal carcinoids form the group of midgut carcinoids that include the classical serotonin producing carcinoids, which represent the most common form of small bowel carcinoids. The majority of jejunal and ileal carcinoids are classic serotonin-producing EC cell carcinoids, and they occur more frequently in the distal

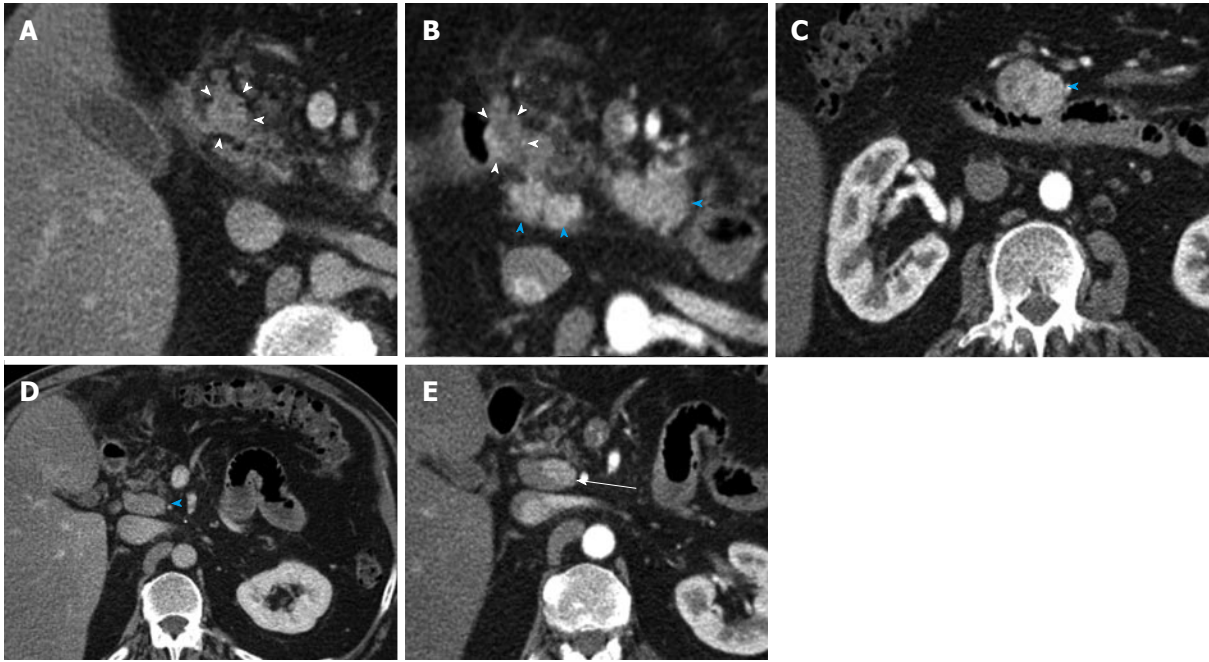


Figure 4 Duodenal Carcinoid. A 61-year-old male with duodenal carcinoid, status-post exploratory laparotomy for a mesenteric mass at an outside institution. Subsequent Whipple procedure demonstrated a 1.8 cm unifocal duodenal carcinoid (pT3, invading pancreas), with 6 of 15 regional lymph node metastases (pN1). This case illustrates the distinction of the primary mass from adjacent nodal metastatic disease and poses an example for nodal metastatic disease having a much larger volume than the primary tumor. A: Venous phase axial computed tomography image shows a 1.8 cm mass in the medial wall of the duodenum, extending into the moderately fatty replaced pancreas, compatible with the primary tumor (arrowheads); B: Arterial phase axial image (magnified, similar slice position) demonstrates heterogeneous hypervascularity in the primary tumor (arrowheads). Multiple metastatic hypervascular peripancreatic lymph nodes are present (blue arrowheads); C: Arterial phase axial image shows a large hypervascular nodal metastasis in the inferior pancreatic groove (blue arrowhead); D: Axial venous phase image shows an enlarged portocaval lymph node (arrowhead); E: Note that in the same node on arterial phase axial image a left-sided hypervascular metastasis can be identified, which was not discernible on the venous phase (D) (arrow).

ileum, reflecting the natural abundance of serotonin-producing EC-cells^[10]. These carcinoids are most commonly malignant, and commonly present with lymph node and liver metastases. There is no significant gender predilection. The mean age at diagnosis is 65 years. The tumors are often asymptomatic during their early stages, during which the liver metabolizes the hormonally active substances until local spread or liver metastases occur. Unless detected incidentally, tumors present either with complications of the primary tumor spread or of metastatic disease. Primary tumor complications are most frequently small intestinal obstruction, bowel ischemia or gastrointestinal bleeding. However, typically the primary tumor is small, commonly below 3.5 cm, and metastatic lesions are found to be significantly larger. Small intramural lesions may occur. Polypoid intraluminal lesions may form lead points for intussusceptions. Characteristically, tumors tend to infiltrate through the bowel wall into the subserosa and the adjacent mesentery, leading to a desmoplastic reaction with kinking, retraction and angulation of the adjacent bowel. Typical metastatic sites of jejunal and ileal carcinoids are locoregional lymph nodes, the mesentery and the liver, and these types of metastases are present in 65% of patients at diagnosis. Thirty percent of jejunal and ileal carcinoids are multiple at diagnosis.

IMAGING OF SMALL BOWEL CARCINOID TUMORS

Scan protocols, data acquisition and image interpretation

Volume acquisition with thin collimation (0.5–1 mm) is preferred for all phases, and provided at our institution by a 64-slice CT scanner (Somatom Sensation 64, Siemens Healthcare).

Typical scan parameters include a tube voltage of 120 kVp, with an effective tube current of 120–160 effective mAs [adjusted in real time by automatic tube current modulation (Care dose, Siemens Healthcare)], gantry rotation time of 0.5 s, beam pitch of 1.2 and table speed of 46 mm per gantry rotation. The resulting submillimeter isotropic dataset is suitable for high quality multiplanar reformations and 3D analysis. CT enterography requires optimal patient preparation with neutral endoluminal contrast. We use a total of 1350 mL of a barium sulfate suspension (VoLumen, Bracco Diagnostics, Monroe Township, NJ, United States) split into three doses of 450 mL each to be administered slowly orally in 10 min intervals before the start of the scan.

For confident detection of the disease manifestations of small bowel carcinoids, we typically perform a dual-phase CT examination, which includes arterial and venous phase imaging. A good early arterial CT

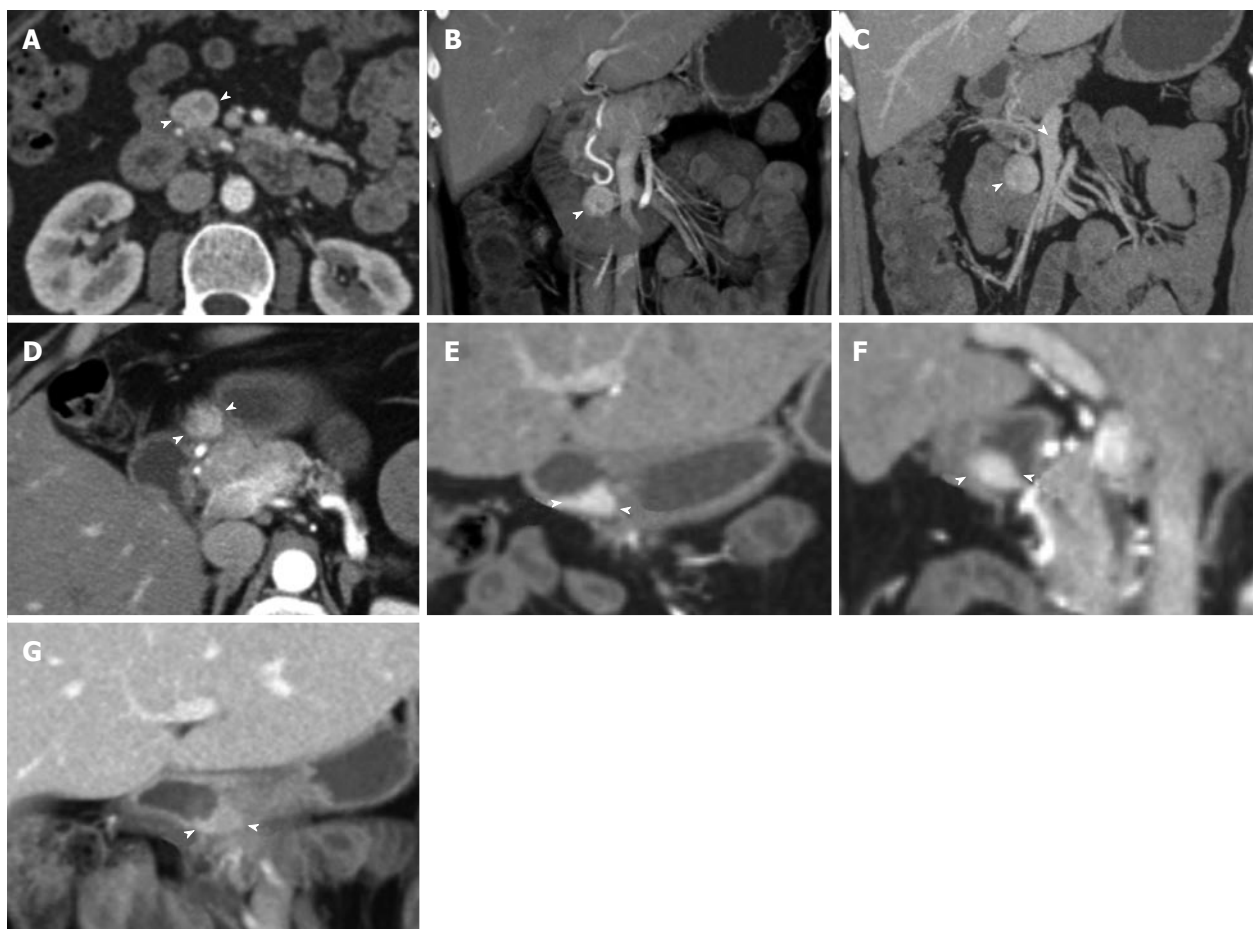


Figure 5 Duodenal carcinoid. Duodenal carcinoid tumor illustrated at two distinct time points. 46-year-old female status-post surgery for removal of an omental carcinoid metastasis, at the first time point presenting with a peripancreatic hypervascular nodal metastasis, which was subsequently surgically removed. A: Axial arterial phase computed tomography (CT) image shows a hypervascular peripancreatic nodal carcinoid metastasis (arrowheads); B: Coronal arterial phase VRT image well demonstrates the location of the hypervascular nodal mass (arrowhead) in the pancreatic groove, abutting the second portion of the duodenum; C: Coronal thick slab MIP image delineates the hypervascular nodal metastasis (arrowhead) in relationship to the SMV (arrow). One year later, at the second time point, a follow-up CT showed appearance of the primary tumor in the duodenal bulb, which was subsequently treated with pancreaticoduodenectomy (Whipple procedure); D, E: Axial (D) and coronal (E) arterial phase CT images show a hyperenhancing mural mass (arrowheads) in the duodenal bulb, just distal to the pylorus, compatible with the patient's primary carcinoid tumor; F: Sagittal arterial phase CT image shows the hyperenhancing mural mass (arrowheads) in the duodenal bulb; G: Coronal arterial phase VRT image demonstrates the intramural hyperenhancing mass (arrowheads). This case illustrates that while the primary tumor may not be initially apparent, it may demarcate itself in the course of the disease, and it also shows the typical imaging appearance of the primary tumor in the form of a hypervascular intramural mass. SMV: Superior mesenteric vein; VRT: Volume rendered technique; MIP: Maximum intensity projections.

angiographic (CTA) imaging acquisition is essential, for which we use a fixed delay of 30 s after start of the intravenous injection. A typical power injection consists of 100-120 mL of nonionic iodinated contrast agent at a rate of 4-5 mL/s.

During image interpretation, axial arterial phase (CTA) images are carefully reviewed for small enhancing bowel lesions. Primary tumors are often small and not well differentiated from bowel wall on the venous phase. Small hyperenhancing masses can still be very inconspicuous on axial images and may be missed if not correlated to multiplanar and 3D analysis.

Multiplanar and 3D analysis consists of volume rendered technique (VRT), multiplanar reconstructions (MPR), maximum intensity projections (MIP) and 3D mapping with surface shading techniques. Figure 1 illustrates how these techniques can supplement the imaging review. Thick slab multiplanar MIP images

support the interactive review by providing a sliding window approach to data review, where small findings are more conspicuous as they appear in a larger number of thick slabs as compared to the review of the individual thin slices. Especially small high contrast structures such as vessels and calcifications are easier to detect and can be shown in contiguity rather than thin interrupted cross-sections. Surface shading is especially useful for the depiction of vessels, specifically of the CTA dataset (Figure 1E). However, interactive choice of the window settings allows the inclusion of variable degrees of soft tissue detail (compare Figure 1A and B). VRT provides depth-encoded shading and is in our experience the best technique to review high contrast vascular, bone and calcified structures together with parenchymal morphology. The relationship between masses and vessels may be easier to discern on VRT (comparison of Figure 1F and G).

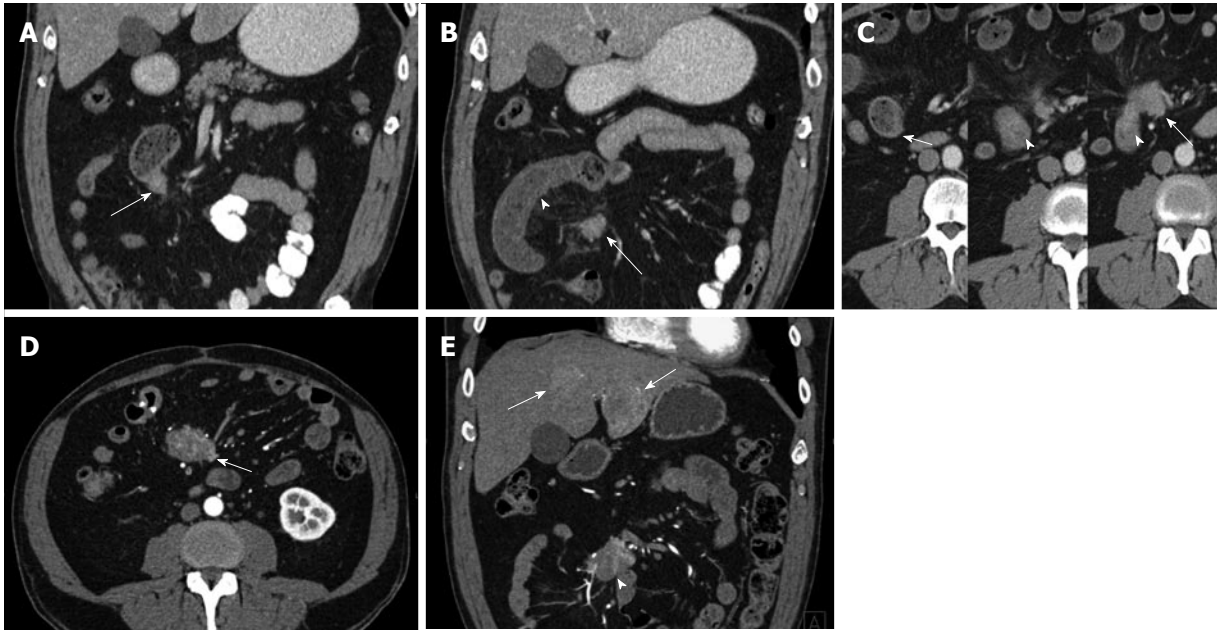


Figure 6 Ileal Carcinoid. A 53-year-old male with stage IV ileal carcinoid tumor, who presented acutely with small bowel obstruction and a history of several months of weight loss, crampy abdominal pain and distention. The patient underwent exploratory laparotomy with surgical resection of an ileal mass (biopsy-proven carcinoid) with primary anastomosis. A large mesenteric mass involving the main superior mesenteric vein and bilateral liver metastases were not resectable. A: Coronal venous phase computed tomography (CT) image shows a hypervascular mass in the wall of a distal ileal loop (arrow) representing the primary carcinoid tumor; B: Coronal venous phase CT image slightly more anterior shows dilated small bowel (arrowhead) with mural thickening and hypoenhancement, compatible with small bowel obstruction and suggestive of hypoperfusion. A portion of a mesenteric nodal mass (arrow) representing regional metastatic disease is shown (arrow); C: Serial axial CT images from the venous phase acquisition; Left: a dilated small bowel loop proximal to the obstruction demonstrates normal bowel wall enhancement and thickness; Middle: Compare the wall thickness and enhancement of the bowel wall at the site of the primary tumor (circumferential mass, invading the mesentery on the left side, arrowhead); Right: The next slice shows the hyperenhancing bowel wall mass (arrowhead) directly abutting the mesenteric lymph nodal metastatic conglomerate mass (arrow); D: Axial arterial phase computed tomography angiography (CTA) image shows the hypervascular mesenteric mass (arrow) reflecting regional lymph node metastatic disease; E: Coronal arterial phase CTA image shows the hypervascular mesenteric mass (arrowhead) reflecting regional lymph node metastatic disease. Hypervascular liver metastases (arrows) are depicted.

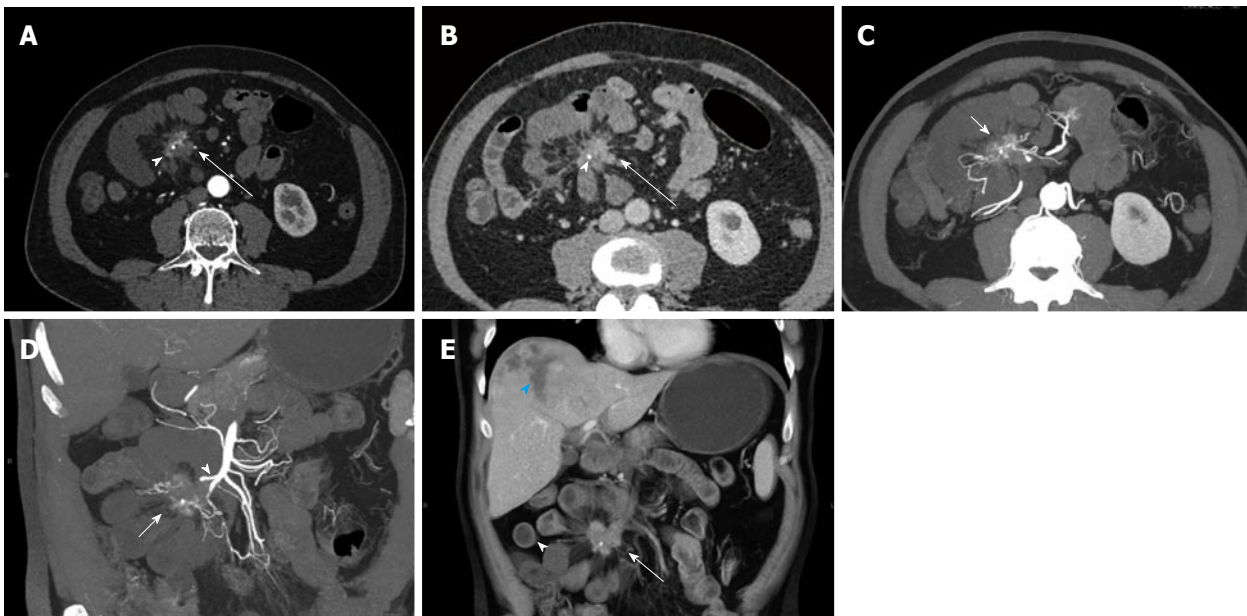


Figure 7 Small bowel carcinoid. A 74-year-old male with small bowel carcinoid (Stage IV), incidentally detected during computed tomography (CT) for presumed kidney stones. He subsequently described a history of flushing and diarrhea, and his urine 5-HIAA level was found elevated. In this case the primary tumor could not be detected on CT. Surgery and pathology demonstrated a polypoid 2 cm mass in the small bowel, likely not detected on CT due to bowel ischemia of the bowel segment involving the tumor. Local nodal metastatic and liver metastatic disease were present. A, B: Axial arterial phase (A) and venous phase (B) images show a hyperenhancing mesenteric mass surrounded by spiculations (arrows) with a small focal calcification (arrowheads), compatible with local nodal metastatic disease with desmoplastic reaction. Multiple dilated small bowel loops with hypoenhancing walls surround the mesenteric mass compatible with the surgical finding of bowel ischemia; C, D: Axial (C) and coronal (D) thick slab MPR images allow the depiction of the relationship of the mesenteric mass (arrows) to the SMA (arrowhead) and the adjacent bowel. The SMA appears irregular and is partially encased by the mass; E: Coronal VRT image allows good visualization of spatial relationships of mesenteric mass (arrow) with calcification, ischemic dilated small bowel loops (arrowhead) and a necrotic liver metastasis in the liver dome (blue arrowhead). VRT: Volume rendered technique; MPR: Multiplanar reconstructions; SMA: Superior mesenteric artery.

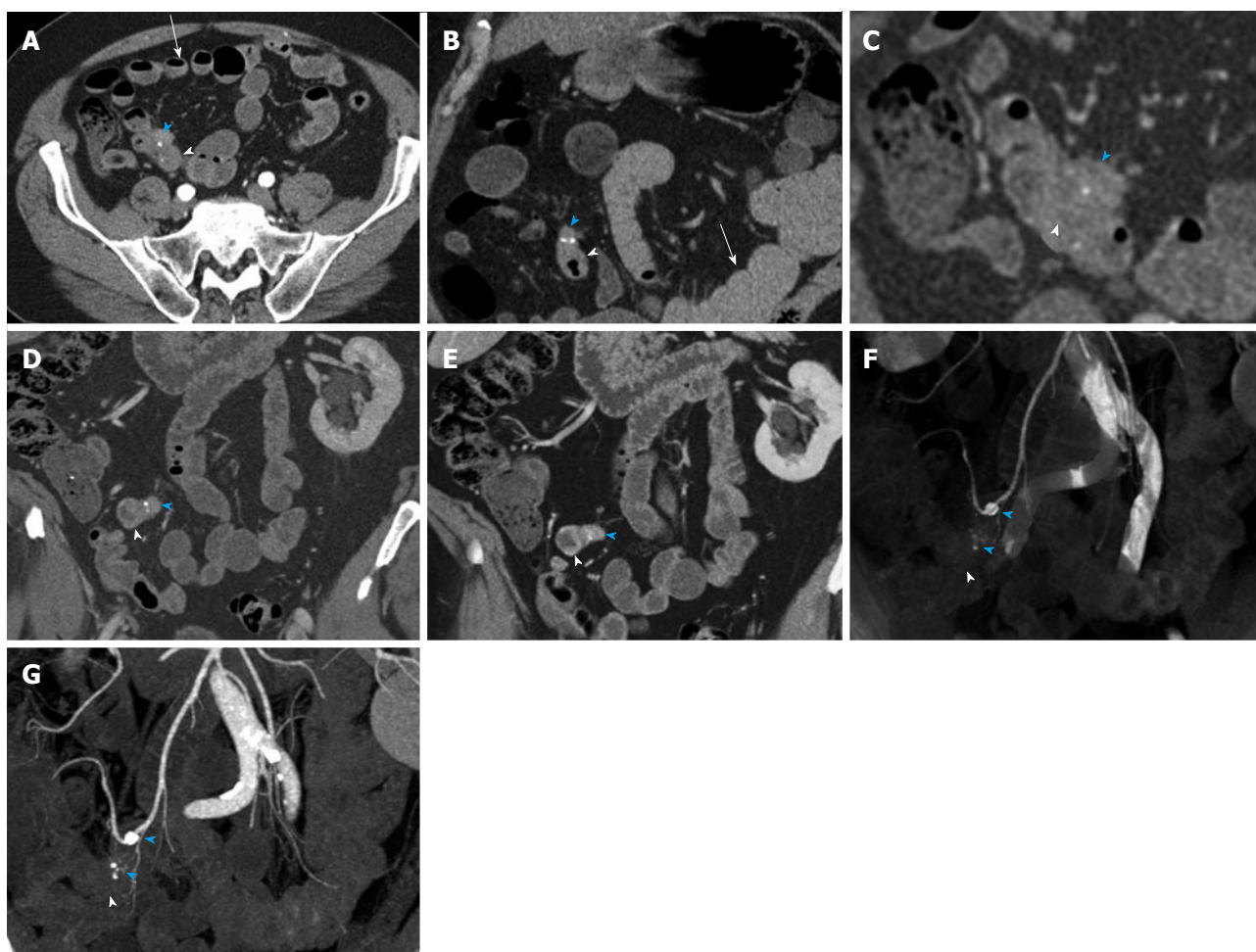


Figure 8 Small bowel carcinoid. A 71-year-old male with small bowel carcinoid, who presented with intermittent abdominal pain and small bowel obstruction. He underwent a 40 cm distal ileal resection, demonstrating a 1.5 cm carcinoid tumor (pT3, invading into subserosal tissue), with regional nodal metastases (2 of 21). After 6 mo of available follow up, there is currently no evidence of metastatic or residual disease. This case illustrates the evaluation of a primary tumor in an underdistended small bowel segment in the setting of small bowel obstruction caused by the mass. Depiction of locoregional metastatic disease. A: Axial arterial phase CTA image shows a small focal area of asymmetric wall thickening in an underdistended small bowel loop (arrowhead), representative of the primary tumor. There is directly adjacent metastatic adenopathy with small calcifications (blue arrowhead). Note that these findings are rather subtle on the axial images. Multiple proximal small bowel loops with fluid levels are compatible with partial small bowel obstruction (arrow). The presence of SBO limits the ability of oral contrast to aid in adequate distention of the pathological small bowel segment; B: Coronal arterial phase image better demonstrates asymmetric wall thickening (arrowhead) and extramural mesenteric extension of tumor with calcifications (blue arrowhead). Multiple dilated proximal small bowel loops are compatible with partial small bowel obstruction (arrow); C: Thin slice reconstructions (0.75 mm) of the venous phase data allow better evaluation of the small bowel mass (arrowhead) and the adjacent calcified mesenteric mass (blue arrowhead); D, E: Coronal thin (D) and thick (E) slab MIP images of the venous phase data demonstrate the small bowel mass (arrowheads) and the adjacent metastatic calcified adenopathy (blue arrowheads) to better advantage; F, G: Coronal VRT (F) and MIP (G) of the CTA data demonstrate the mass (arrowheads) and associated calcified nodal masses (blue arrowheads) in relation to the mesenteric vessels. VRT: Volume rendered technique; MIP: Maximum intensity projections; CTA: Computed tomography angiography. SBO: Small bowel obstruction.

Challenging cases highlighting opportunities and pitfalls in imaging small bowel carcinoid tumors

Characteristic imaging findings of small bowel carcinoid tumors are shown in 14 challenging cases. Cases are ordered in four groups, beginning with duodenal carcinoid and periampullary carcinoid (Figures 2-5), followed by ileal and jejunal carcinoid (Figures 6-10). An example of metastatic carcinoid of unknown primary is shown in Figure 11. Finally, the imaging appearance of recurrent and previously treated small bowel carcinoid tumors is shown (Figures 12-14). Primary tumors may be solitary or multifocal, occur predominantly in the distal ileum and may show evidence of ulceration, in the latter case associated with the classic target sign

on fluoroscopic enteroclysis. If a solitary small bowel mass is found on imaging, the classical differential diagnosis includes small-bowel carcinoid, primary bowel adenocarcinoma, lymphoma, gastrointestinal stromal tumor and mesenchymal neoplasm (*e.g.*, small bowel sarcoma), and non-neoplastic inflammatory bowel disease such as Crohn's disease, which has a propensity to involve the small bowel in the form of skip lesions. Primary carcinoid tumors are classically not well identified on standard venous phase thick section CT and their confident detection is aided by state of the art imaging with volumetric CTA with CT enterography or enteroclysis. Mural thickening is often the earliest, however also an unspecific manifestation

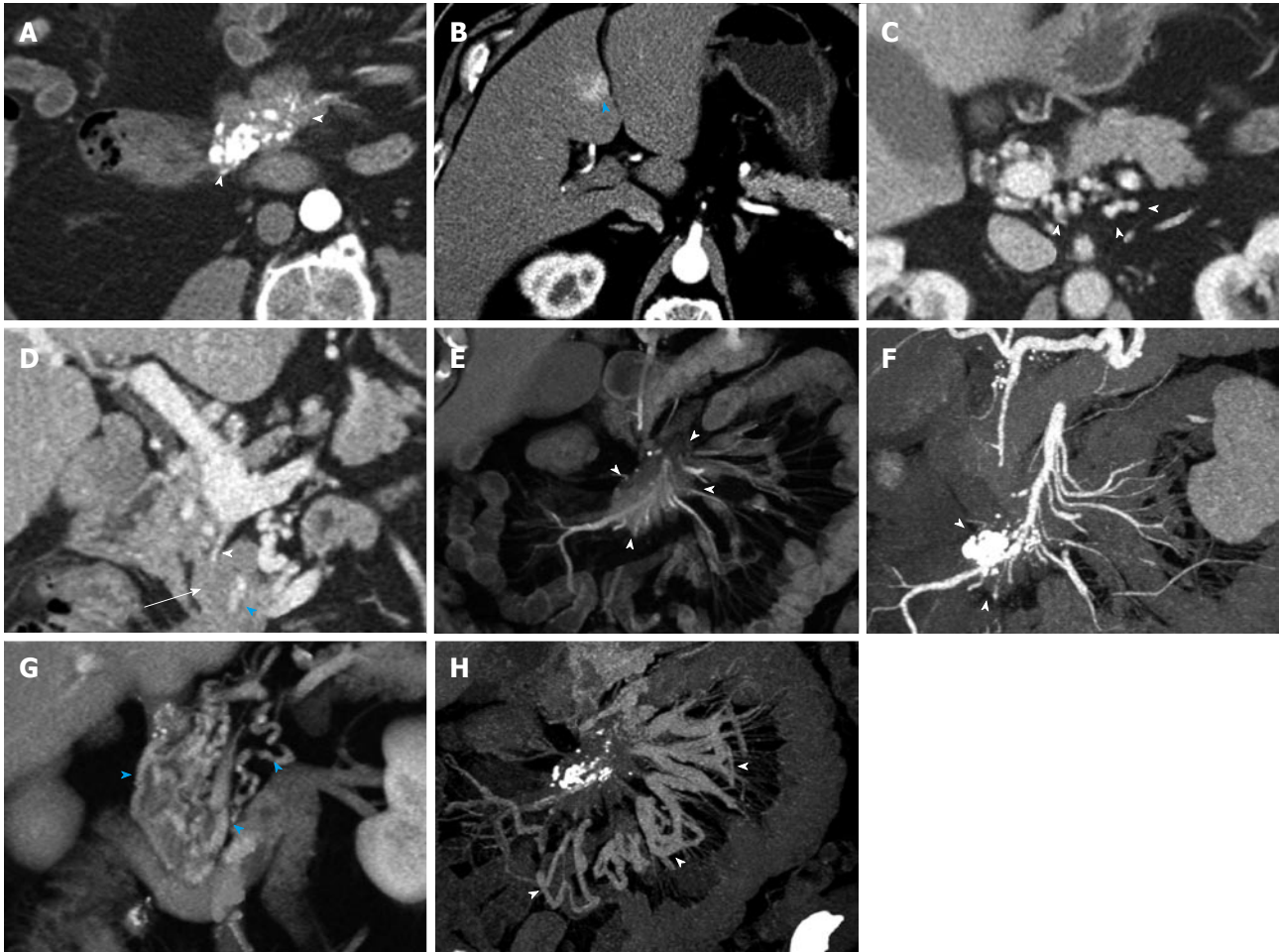


Figure 9 Metastatic small bowel carcinoid. A 66-year-old male with metastatic small bowel carcinoid. The tumor was found unresectable with large mesenteric nodal metastatic disease encasing SMA and SMV, and with liver metastases. In this case the primary tumor location is unknown (and possibly very small), in the presence of bulky regional metastatic disease and liver metastatic disease. It also demonstrates the evaluation of vascular complications (SMV occlusion, encasement of SMV and SMA) using 3D imaging. It is not unusual that the primary tumor is much smaller than the nodal metastatic disease. A: Arterial phase axial image demonstrates a large mesenteric mass with surrounding desmoplastic reaction (arrowheads), compatible with regional nodal metastatic disease from carcinoid tumor. The primary tumor was not identified on the exam; B: Arterial phase axial image demonstrates a hypervascular metastasis in segment IV B of the liver; C: Axial venous phase image shows extensive peripancreatic collateral vessels (arrowheads) as a result of SMV occlusion by tumor encasement; D: Encasement of the SMV (arrowhead) and SMA (blue arrowhead) by the tumor. The distal SMV is severely narrowed (arrowhead), while the more proximal SMV is completely occluded by the tumor (arrow); E: Coronal VRT arterial phase image demonstrates the large mesenteric mass (arrowheads), which encases the SMA and its branches; F: Coronal thick slab MIP arterial phase image demonstrates the calcified mesenteric mass (arrowheads), encasing SMA branches; G: Coronal VRT venous phase image shows multiple peripancreatic collateral vessels (blue arrowheads) to better advantage than axial or multiplanar imaging; H: Coronal thick slab venous phase MIP image shows moderately dilated mesenteric veins (arrowheads) resulting from SMV occlusion. VRT: Volume rendered technique; MIP: Maximum intensity projections; SMA: Superior mesenteric artery; SMV: Superior mesenteric vein.

of small bowel carcinoid tumors^[10,20,34]. Primary tumors are not uncommonly small, often less than 2 cm. Characteristically, the primary tumor may be notably smaller than the mesenteric and nodal disease (Figure 4B). Especially if the primary tumor is not notably hypervascular, it can be very inconspicuous in underdistended bowel segments^[34,35]. While good bowel distention can be achieved by proper bowel preparation in otherwise healthy patients with small non-obstructing tumors, if small bowel obstruction is present, an evaluation for the location and size of the primary tumor in the presence of underdistended small bowel can often not be avoided (Figure 8). Focal bowel wall thickening can provide a clue that leads to further evaluation of a specific area. A characteristic appearance of a submucosal mass with extramural extension

and mesenteric disease in underdistended bowel in the setting of bowel obstruction is shown in Figure 6. Not uncommonly, the primary tumor site is located in proximity to the lead point of the bowel obstruction. Even with high resolution submillimeter isotropic CT enterography or enteroclysis, primary tumors less than 10 mm in size can be missed in 14% of patients even with excellent technique and patient preparation^[20]. While initial reports using CT protocols without specific bowel preparation were able to detect less than half of the primary tumors seen at surgery^[34], CT enteroclysis has recently shown a high sensitivity (up to 93%) in the detection of small bowel tumors^[35-38]. Small primary tumors may present as a well-defined polypoid mass in mucosal or submucosal location, often with associated hyperenhancement (Figures 2, 3A, 5 and

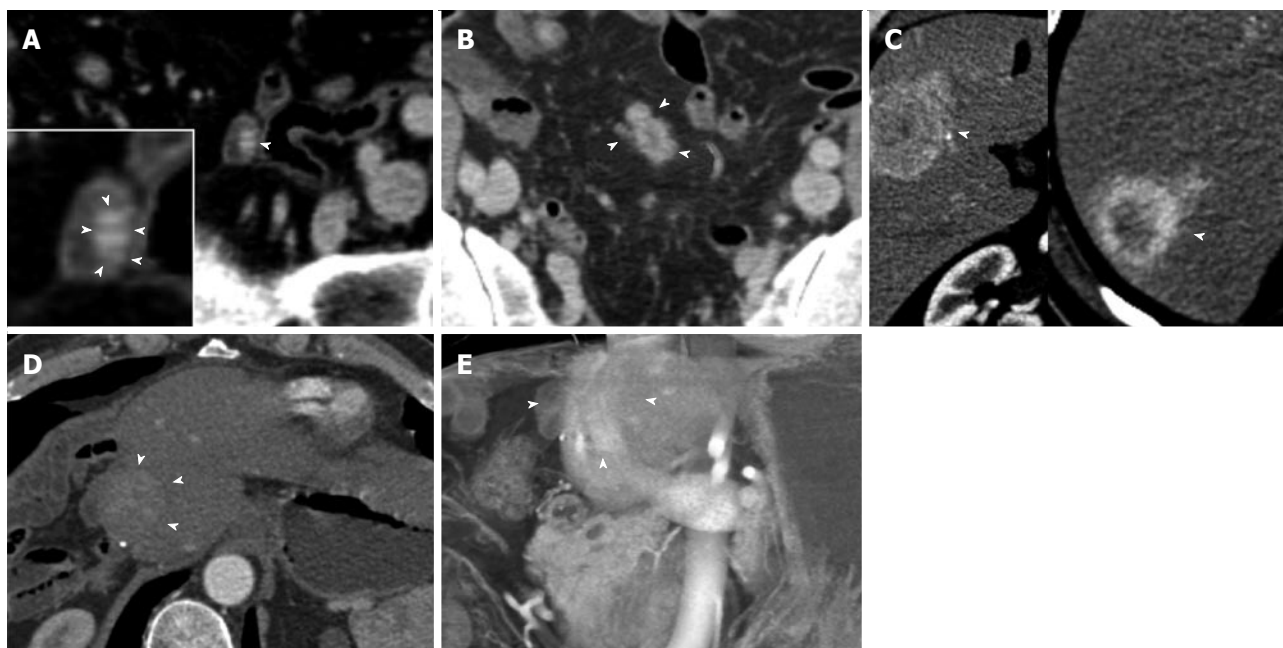


Figure 10 Metastatic terminal ileal carcinoid. Terminal ileal small bowel carcinoid tumor with liver metastases. A 57-year-old male with longstanding history of flushing, diarrhea and sweating. Three hypervascular hepatic metastases were found during a computed tomography (CT) evaluation performed after he presented with a diverticular perforation to an outside institution. A Hartmann procedure was performed. After diagnosis, he underwent an extended right hemihepatectomy. An ileal resection proved a terminal ileal 1.5 cm primary carcinoid tumor. Four years later, he presented with a recurrence at the liver resection margin. This case illustrates the imaging appearance of the primary tumor as a hypervascular mural mass and extensive locoregional nodal metastatic and liver metastatic disease despite a small (1.5 cm) primary tumor. A: Axial venous phase CECT demonstrates a small bowel loop (terminal ileum) with a small hyperenhancing mural mass (arrowhead). A detail view better demonstrates the mass (inset, arrowheads), which represents the primary tumor and was confirmed at surgery. The primary tumor is subtle and easily missed on the axial CT slices; B: Axial venous phases CECT image slightly superiorly demonstrates matted hypervascular mesenteric lymph node metastases with minimal surrounding desmoplastic reaction (arrowheads), typical for carcinoid tumor local metastases; C: Axial arterial phase images demonstrate segment VIII/V (left) and segment VII (right) hypervascular, centrally necrotic liver metastases (arrowheads). Note that this advanced disease is associated with the small (1.5 cm) primary tumor. It is not uncommon that metastatic disease is significantly larger than the primary carcinoid tumor; D, E: Follow-up exam 4 years after extended right hepatectomy shows recurrence at the resection margin (arrowheads), shown on the axial venous phase image (D) and a coronal volume rendered technique image (E). CETC: Contrast enhanced computed tomography.

10A). A duodenal carcinoid tumor may be imaged as a periampullary mass with biliary and pancreatic ductal obstruction (Figure 3). Not always is the primary tumor found on initial imaging or initial surgery. In these cases the patient may undergo resection of limited metastatic disease. On imaging follow-up, evaluation should focus not only on the detection of recurrent or progressive metastatic disease, but also observe the first imaging manifestation of a previously occult primary small bowel carcinoid tumor (Figure 5).

Once extramural extension occurs, the segmental morphology of the bowel may be altered. A hairpin turn morphology (a fixed narrow turn or kink of the bowel) or angulation reflects underlying bowel infiltration and fibrosis, which may itself be subtle on imaging. Transmural tumor extension may manifest itself as concentric wall thickening, or as a focal soft-tissue mass transgressing the bowel wall (Figure 6C)^[39]. Small bowel carcinoids may also exhibit primarily a diffuse infiltrative growth pattern, in which case only bowel wall thickening and desmoplastic reaction may be observable. The tumor itself typically shows associated contrast enhancement, while the surrounding desmoplastic reaction will appear as a slowly enhancing spiculated mass (Figures 7A and 11). Carcinoid tumors have a propensity to encase and occlude large, medium

and small vessels, related to fibrosis and their secretion of vasoactive substances, with the possible result of an interruption of blood supply to the bowel and subsequent bowel ischemia^[40]. The typical imaging appearance of arterial encasement, arterial narrowing and arterial caliber irregularities is shown in Figures 9 and 12. An example of venous encasement leading to occlusion of the superior mesenteric vein with the formation of peripancreatic collateral vessels and engorgement of the mesenteric vein arcades is depicted in Figure 9. The surrounding bowel is not uncommonly thickened (with preserved wall enhancement) as a result of chronic venous and lymphatic obstruction secondary to the mesenteric mass. In addition to small bowel obstruction which often accompanies small bowel ischemia, the additional lack of contrast enhancement of the affected bowel segments combined with edematous bowel wall thickening will make detection of the primary tumor more difficult (Figure 7). Frank acute bowel ischemia is relatively uncommon due to the relatively slow involvement by the tumor of the adjacent vasculature, but ischemia should be suspected if bowel wall thickening is found in combination with lack of enhancement or hypoenhancement of the bowel wall.

As the primary tumor may be difficult to detect and may remain occult even on repeat imaging, the



Figure 11 Carcinoid of unknown primary. Functional carcinoid tumor of unknown primary, metastatic to liver and mesenteric root. A 43-year-old female with history of postprandial nausea. Ultrasound exam detected bilobar liver metastases. Subsequent computed tomography (CT) demonstrated hypervascularity of the liver metastases. Liver biopsy confirmed carcinoid metastases. She underwent systemic chemotherapy with VP-16 and carboplatin and locoregional therapy to the liver metastases (Yttrium-90 microsphere embolization). This case illustrates the evaluation of and appearance of locoregional nodal metastatic and liver metastatic disease. A: Axial arterial phase CT shows multiple hypervascular liver metastases with treatment changes after chemoembolization (arrowheads) and diffuse perfusion change in the left liver lobe related to prior locoregional therapy; B: Axial arterial phase CT image shows a hypervascular mesenteric mass (arrowhead) compatible with metastatic nodal disease; C: Coronal thick slab MIP image demonstrates the hypervascular mesenteric mass (arrow) and its relationship to the SMA and portal vein (arrowhead); D: Coronal VRT image demonstrates hypervascular liver metastasis (arrowhead) and mesenteric mass (arrow). The extensive desmoplastic reaction surrounding the mesenteric mass is well shown. VRT: Volume rendered technique; MIP: Maximum intensity projections; SMA: Superior mesenteric artery.

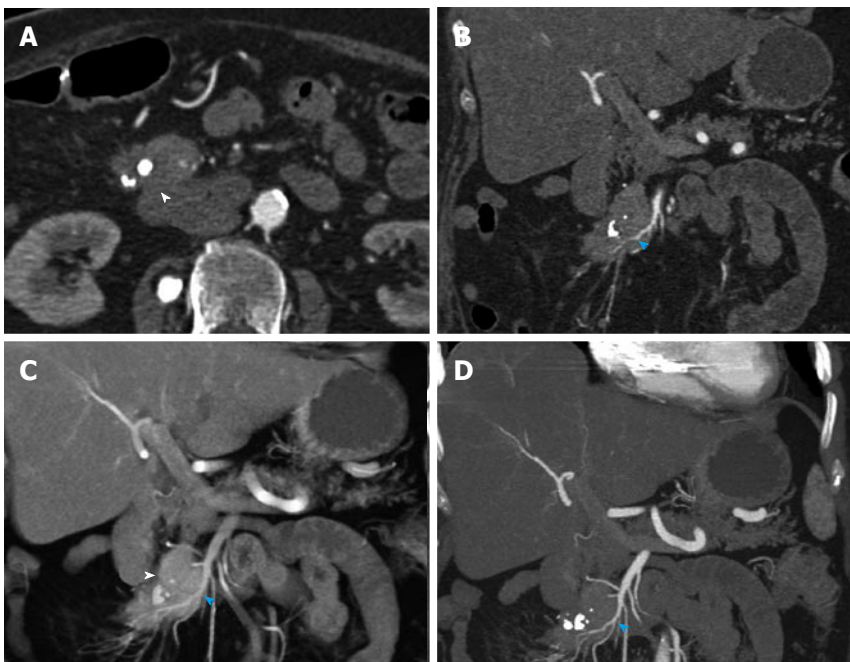


Figure 12 Recurrent metastatic small bowel carcinoid. A 72-year-old female with metastatic small bowel carcinoid. She underwent right hemicolectomy and partial small bowel resection 10 years ago, and is currently on long-acting octreotide. This case illustrates the imaging appearance and evaluation of mesenteric locoregional nodal metastatic disease recurrence with 3D imaging. A: Axial arterial phase imaging shows a calcified mass in the mesentery (arrowhead) compatible with recurrent metastatic carcinoid tumor; B: Coronal CTA image shows encasement of branches of superior mesenteric artery (blue arrowhead), with associated luminal irregularities and narrowing of the artery; C: Coronal VRT image depicts the calcified mass (arrowhead) and allows analysis of the morphology of the SMA branches within and distal to the tumor. Encased SMA branches demonstrate luminal narrowing and irregularity (blue arrowhead); D: Thick slab coronal MIP is of high diagnostic value in this case, as it benefits from the excellent contrast between vascular lumen and tumor tissue, probably providing the best assessment of the morphology of the encased SMA branches (blue arrowhead). VRT: Volume rendered technique; MIP: Maximum intensity projections; SMA: Superior mesenteric artery.



Figure 13 Recurrent metastatic small bowel carcinoid. 52-year-old male with metastatic small bowel carcinoid. He presented for follow-up one year after small bowel resection for carcinoid tumor. This case illustrates the imaging appearance of recurrent locoregional nodal metastatic disease. Axial arterial phase axial images show a small mass in the small bowel mesentery (arrowhead) with surrounding mild desmoplastic reaction, compatible with recurrence of metastatic carcinoid tumor. A surgical small bowel anastomosis is noted (blue arrowhead).

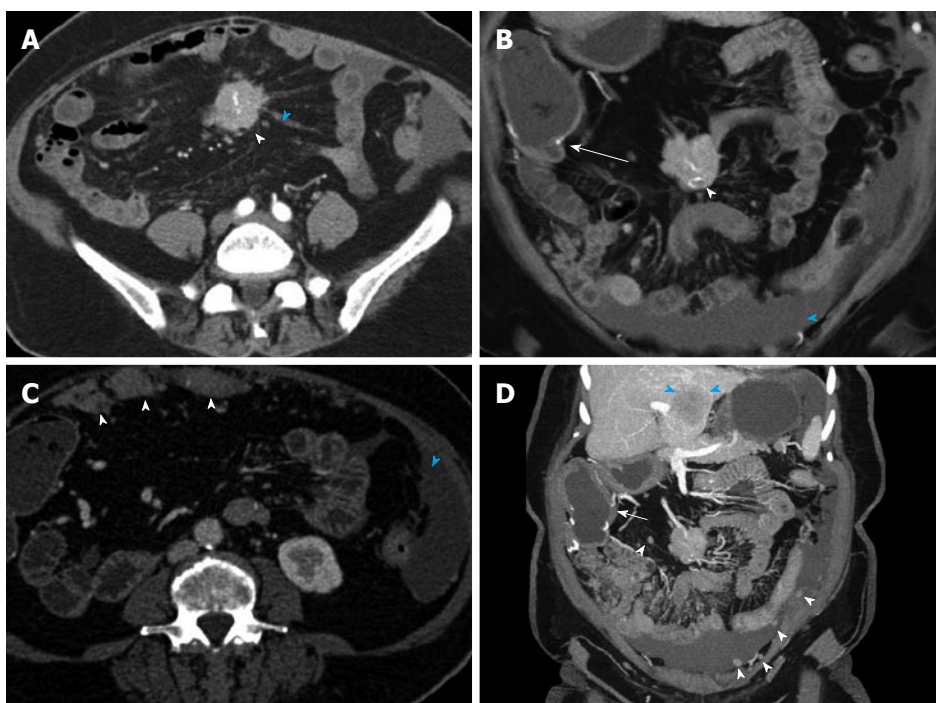


Figure 14 Recurrent metastatic small bowel carcinoid. 71-year-old female with metastatic small bowel carcinoid. Twelve years ago she had undergone a segmental distal ileal resection and liver segmental resection for metastatic carcinoid. This case illustrates advanced recurrent metastatic carcinoid with extensive abdominal and pelvic peritoneal implants and hepatic metastatic disease. A: Axial arterial phase axial image shows a calcified mass in the small bowel mesentery (arrowhead) with surrounding linear desmoplastic reaction (blue arrowhead), compatible with carcinoid tumor metastasis; B: Coronal arterial phase VRT image shows the calcified mesenteric mass (arrowhead). The patient is status post terminal ileal and proximal colonic resection with ileocolic anastomosis (arrow). Moderate ascites is present (blue arrowhead); C: Axial arterial phase axial image shows multiple metastatic omental implants (arrowheads). Ascites is present (open arrowhead); D: Many additional omental implants are noted (arrowheads) on this coronal thick slab MIP image. Ileocolic anastomosis and colonic thickening (arrow) in the setting of ascites are noted. Large segment IVB liver metastasis (blue arrowheads). VRT: Volume rendered technique; MIP: Maximum intensity projections.

diagnosis of small bowel carcinoids is not uncommonly made on the basis of secondary tumor manifestations. The main secondary manifestations of locoregional tumor spread include locoregional and mesenteric disease, and distant metastases. Duodenal carcinoid tumor metastases may cause peripancreatic (Figure 5) or portocaval metastatic adenopathy (Figure 4). Mesenteric disease characteristically leads to desmoplastic reaction surrounding the metastatic lesions, appearing as mesenteric retraction, spiculation

and tethering of adjacent bowel loops (Figures 9 and 12). The desmoplastic reaction in itself reflects fibrosis, but may also contain diffuse infiltration by tumor cells. Usually centrally embedded in the desmoplastic reaction lies matted carcinoid-related mesenteric nodal metastatic disease, which can be calcified in up to 70% of cases, and not uncommonly demonstrates avid contrast enhancement^[41-44]. The identification of a stellate configuration of radiating strands of fibrosis in the mesentery surrounding an enhancing calcified

mesenteric mass that itself is detached from the bowel wall is nearly pathognomonic for locoregionally metastatic carcinoid tumor (Figure 7)^[41,45]. The main alternative differential considerations of treated lymphoma and retractile or sclerosing mesenteritis can usually be differentiated by clinical history, additional imaging findings and laboratory testing. The location can also be very helpful in such cases, as mesenteric carcinoid in most cases is located in the right lower quadrant ileal mesentery, while calcified retractile mesenteritis is most often located in the jejunal mesentery in the left upper quadrant. Rarely, carcinoid metastases may cause diffuse mesenteric and peritoneal disease with miliary peritoneal implants, omental or mesenteric caking, or large mesenteric masses (Figure 14). Distant metastatic disease occurs most frequently to the liver, where liver metastases characteristically appear hypervascular (Figures 9 and 11), and are well depicted in the arterial phase, although larger liver metastases may exhibit central hypoenhancement due to necrosis (Figure 10C).

After surgical resection, common sites of disease recurrence include locoregional and nodal disease recurrence, *e.g.*, in the form of a mesenteric mass (Figure 13), demarcation of a previously occult primary carcinoid (Figure 5), recurrence at the hepatic resection margin after surgical partial hepatectomy for distant metastatic disease (Figure 10D and E), and omental and peritoneal dissemination (Figure 14).

CONCLUSION

3D CT and CTA of small bowel carcinoid tumors with CT enterography provides many opportunities in the early detection of small bowel carcinoids. The most important factors for the optimal detection of the often small hypervascular primary tumor are the use of a negative endoluminal contrast agent with good distention of the small bowel, and the utilization of an optimal multi-detector computed tomography (MDCT) scan protocol at submillimeter resolution with the acquisition of good CTA and venous phase data^[35,42]. Optimal bowel distention is necessary to detect submucosal masses and determine the endoluminal morphology of the small bowel, while a good CTA acquisition and high-resolution data allow the detection of hyperenhancement even of very small lesions. Extraluminal disease, such as the extent of bowel wall invasion, desmoplastic reaction and local and distal metastatic disease, together with their effects on the arterial and venous supply can be evaluated with a high degree of confidence by reviewing the high resolution multiphase MDCT data with the utilization of MIP, MPR, VRT and surface shading techniques. Spatial resolution is the main determinant of small lesion detection, accompanied by scan speed which helps to reduce motion artifacts that may otherwise blur small lesions. Faster scanners and higher spatial resolution are therefore expected to detect smaller lesions in the

future, helped by a further increase in the quality of the resulting 3D techniques. The higher speed of acquisition and higher isotropic spatial coverage of modern MDCT are also advantages over current magnetic resonance imaging techniques such as MR enterography and diffusion-weighted imaging^[46]. The arterial phase highlights the typical hypervascularity of the primary tumor, nodal metastatic disease and liver and peritoneal metastases. The patients discussed above were examined with a CT enterography technique that does not require the placement of a duodenal catheter as typically used for CT enteroclysis. CT enterography has the advantage of higher patient comfort during the study and during the fluoroscopically guided catheter placement, while the enterographic technique provides high quality imaging of the small bowel mucosal surface compared to standard abdominal CT protocols. While overall better bowel distention may be achieved by enterodysis^[15,47], in our experience, the CT enterography protocol achieves good bowel distention in most patients. As shown in the cases, patients may present emergently with bowel obstruction or ischemia, leading to an unavoidably limited luminal evaluation. While small tumors can remain a diagnostic challenge, if all the above criteria are met, CT can have high accuracy in the diagnosis of carcinoid tumors.

REFERENCES

- 1 **Bader TR**, Semelka RC, Chiu VC, Armao DM, Woosley JT. MRI of carcinoid tumors: spectrum of appearances in the gastrointestinal tract and liver. *J Magn Reson Imaging* 2001; **14**: 261-269 [PMID: 11536403 DOI: 10.1002/jmri.1182]
- 2 **Modlin IM**, Lye KD, Kidd M. A 5-decade analysis of 13,715 carcinoid tumors. *Cancer* 2003; **97**: 934-959 [PMID: 12569593 DOI: 10.1002/cncr.11105]
- 3 **Levy AD**, Sobin LH. From the archives of the AFIP: Gastrointestinal carcinoids: imaging features with clinicopathologic comparison. *Radiographics* 2007; **27**: 237-257 [PMID: 17235010 DOI: 10.1148/rg.271065169]
- 4 **Modlin IM**, Oberg K, Chung DC, Jensen RT, de Herder WW, Thakker RV, Caplin M, Delle Fave G, Kaltsas GA, Krenning EP, Moss SF, Nilsson O, Rindi G, Salazar R, Ruzsniwski P, Sundin A. Gastroenteropancreatic neuroendocrine tumours. *Lancet Oncol* 2008; **9**: 61-72 [PMID: 18177818 DOI: 10.1016/S1470-2045(07)70410-2]
- 5 **Pinchot SN**, Holen K, Sippel RS, Chen H. Carcinoid tumors. *Oncologist* 2008; **13**: 1255-1269 [PMID: 19091780 DOI: 10.1634/theoncologist.2008-0207]
- 6 **Moran CA**, Suster S. Neuroendocrine carcinomas (carcinoid, atypical carcinoid, small cell carcinoma, and large cell neuroendocrine carcinoma): current concepts. *Hematol Oncol Clin North Am* 2007; **21**: 395-407; vii [PMID: 17548031 DOI: 10.1016/j.hoc.2007.04.011]
- 7 **Wallace S**, Ajani JA, Charnsangavej C, DuBrow R, Yang DJ, Chuang VP, Carrasco CH, Dodd GD. Carcinoid tumors: imaging procedures and interventional radiology. *World J Surg* 1996; **20**: 147-156 [PMID: 8661810 DOI: 10.1007/s002689900023]
- 8 **Crocetti E**, Paci E. Malignant carcinoids in the USA, SEER 1992-1999. An epidemiological study with 6830 cases. *Eur J Cancer Prev* 2003; **12**: 191-194 [PMID: 12771556 DOI: 10.1097/01.cej.0000072851.07402.96]
- 9 **Gore RM**, Mehta UK, Berlin JW, Rao V, Newmark GM. Diagnosis and staging of small bowel tumours. *Cancer Imaging* 2006; **6**: 209-212 [PMID: 17208678 DOI: 10.1102/1470-7330.2006.0031]

- 10 **Buck JL**, Sobin LH. Carcinoids of the gastrointestinal tract. *Radiographics* 1990; **10**: 1081-1095 [PMID: 2259762 DOI: 10.1148/radiographics.10.6.2259762]
- 11 **Frilling A**, Akerström G, Falconi M, Pavel M, Ramos J, Kidd M, Modlin IM. Neuroendocrine tumor disease: an evolving landscape. *Endocr Relat Cancer* 2012; **19**: R163-R185 [PMID: 22645227 DOI: 10.1530/ERC-12-0024]
- 12 **Modlin IM**, Kidd M, Latich I, Zikusoka MN, Shapiro MD. Current status of gastrointestinal carcinoids. *Gastroenterology* 2005; **128**: 1717-1751 [PMID: 15887161 DOI: 10.1053/j.gastro.2005.03.038]
- 13 **Klöppel G**, Anlauf M. Epidemiology, tumour biology and histopathological classification of neuroendocrine tumours of the gastrointestinal tract. *Best Pract Res Clin Gastroenterol* 2005; **19**: 507-517 [PMID: 16183524 DOI: 10.1016/j.bpg.2005.02.010]
- 14 **Mocellin S**, Nitti D. Gastrointestinal carcinoid: epidemiological and survival evidence from a large population-based study (n = 25 531). *Ann Oncol* 2013; **24**: 3040-3044 [PMID: 24050954 DOI: 10.1093/annonc/mdt377]
- 15 **Kamaoui I**, De-Luca V, Ficarelli S, Mennesson N, Lombard-Bohas C, Pilleul F. Value of CT enteroclysis in suspected small-bowel carcinoid tumors. *AJR Am J Roentgenol* 2010; **194**: 629-633 [PMID: 20173138 DOI: 10.2214/AJR.09.2760]
- 16 **Verma D**, Strohlein JR. Adenocarcinoma of the small bowel: a 60-yr perspective derived from M. D. Anderson Cancer Center Tumor Registry. *Am J Gastroenterol* 2006; **101**: 1647-1654 [PMID: 16863573 DOI: 10.1111/j.1572-0241.2006.00625.x]
- 17 **Dierdorf SF**. Carcinoid tumor and carcinoid syndrome. *Curr Opin Anaesthesiol* 2003; **16**: 343-347 [PMID: 17021482 DOI: 10.1097/0001503-200306000-00017]
- 18 **Thomas AM**, Beumer JD, Suppiah A, Devitt PG.. Unusual cause of gastrointestinal bleeding: multiple small bowel carcinoid tumours. *ANZ J Surg* 2014; Epub ahead of print [PMID: 25251986 DOI: 10.1111/ans.12853]
- 19 **Caracappa D**, Gullà N, Lombardo F, Burini G, Castellani E, Boselli C, Gemini A, Burattini MF, Covarelli P, Noya G. Incidental finding of carcinoid tumor on Meckel's diverticulum: case report and literature review, should prophylactic resection be recommended? *World J Surg Oncol* 2014; **12**: 144 [PMID: 24884768 DOI: 10.1186/1477-7819-12-144]
- 20 **Datta S**, Williams N, Suortamo S, Mahmood A, Oliver C, Hedley N, Ray P. Carcinoid syndrome from small bowel endocrine carcinoma in the absence of hepatic metastasis. *Age Ageing* 2011; **40**: 760-762 [PMID: 21903639 DOI: 10.1093/ageing/afr122]
- 21 **Klöppel G**, Perren A, Heitz PU. The gastroenteropancreatic neuroendocrine cell system and its tumors: the WHO classification. *Ann N Y Acad Sci* 2004; **1014**: 13-27 [PMID: 15153416 DOI: 10.1196/annals.1294.002]
- 22 **Burke AP**, Thomas RM, Elsayed AM, Sobin LH. Carcinoids of the jejunum and ileum: an immunohistochemical and clinicopathologic study of 167 cases. *Cancer* 1997; **79**: 1086-1093 [PMID: 9070484 DOI: 10.1002/(SICI)1097-0142(19970315)79]
- 23 **Eller R**, Frazee R, Roberts J. Gastrointestinal carcinoid tumors. *Am Surg* 1991; **57**: 434-437 [PMID: 2058850]
- 24 **Strodel WE**, Talpos G, Eckhauser F, Thompson N. Surgical therapy for small-bowel carcinoid tumors. *Arch Surg* 1983; **118**: 391-397 [PMID: 6830429 DOI: 10.1001/archsurg.1983.01390040003001]
- 25 **Thompson GB**, van Heerden JA, Martin JK, Schutt AJ, Ilstrup DM, Carney JA. Carcinoid tumors of the gastrointestinal tract: presentation, management, and prognosis. *Surgery* 1985; **98**: 1054-1063 [PMID: 4071383]
- 26 **Toumpanakis C**, Caplin ME. Update on the role of somatostatin analogs for the treatment of patients with gastroenteropancreatic neuroendocrine tumors. *Semin Oncol* 2013; **40**: 56-68 [PMID: 23391113 DOI: 10.1053/j.seminoncol.2012.11.006]
- 27 **Godwin JD**. Carcinoid tumors. An analysis of 2,837 cases. *Cancer* 1975; **36**: 560-569 [PMID: 1157019 DOI: 10.1002/1097-0142(197508)36]
- 28 **Addiss DG**, Shaffer N, Fowler BS, Tauxe RV. The epidemiology of appendicitis and appendectomy in the United States. *Am J Epidemiol* 1990; **132**: 910-925 [PMID: 2239906]
- 29 **Hemminki K**, Li X. Incidence trends and risk factors of carcinoid tumors: a nationwide epidemiologic study from Sweden. *Cancer* 2001; **92**: 2204-2210 [PMID: 11596039]
- 30 **Ellis L**, Shale MJ, Coleman MP. Carcinoid tumors of the gastrointestinal tract: trends in incidence in England since 1971. *Am J Gastroenterol* 2010; **105**: 2563-2569 [PMID: 20823835 DOI: 10.1038/ajg.2010.341]
- 31 **Yao JC**, Hassan M, Phan A, Dagohoy C, Leary C, Mares JE, Abdalla EK, Fleming JB, Vauthey JN, Rashid A, Evans DB. One hundred years after "carcinoid": epidemiology of and prognostic factors for neuroendocrine tumors in 35,825 cases in the United States. *J Clin Oncol* 2008; **26**: 3063-3072 [PMID: 18565894 DOI: 10.1200/JCO.2007.15.4377]
- 32 **Fitzgerald TL**, Dennis SO, Kachare SD, Vohra NA, Zervos EE. Increasing incidence of duodenal neuroendocrine tumors: Incidental discovery of indolent disease? *Surgery* 2015; **158**: 466-471 [PMID: 26013986 DOI: 10.1016/j.surg.2015.03.042]
- 33 **Hodgson N**, Koniaris LG, Livingstone AS, Franceschi D. Gastric carcinoids: a temporal increase with proton pump introduction. *Surg Endosc* 2005; **19**: 1610-1612 [PMID: 16211437 DOI: 10.1007/s00464-005-0232-4]
- 34 **Picus D**, Glazer HS, Levitt RG, Husband JE. Computed tomography of abdominal carcinoid tumors. *AJR Am J Roentgenol* 1984; **143**: 581-584 [PMID: 6331739 DOI: 10.2214/ajr.143.3.581]
- 35 **Soyer P**, Boudiaf M, Fishman EK, Hoeffel C, Dray X, Manfredi R, Marteau P. Imaging of malignant neoplasms of the mesenteric small bowel: new trends and perspectives. *Crit Rev Oncol Hematol* 2011; **80**: 10-30 [PMID: 21035353 DOI: 10.1016/j.critrevonc.2010.09.010]
- 36 **Soyer P**, Aout M, Hoeffel C, Vicaute E, Placé V, Boudiaf M. Helical CT-enteroclysis in the detection of small-bowel tumours: a meta-analysis. *Eur Radiol* 2013; **23**: 388-399 [PMID: 22865269 DOI: 10.1007/s00330-012-2595-y]
- 37 **Maglente DD**, Sandrasegaran K, Lappas JC, Chiorean M. CT Enteroclysis. *Radiology* 2007; **245**: 661-671 [PMID: 18024448 DOI: 10.1148/radiol.2453060798]
- 38 **Soyer P**. Obscure gastrointestinal bleeding: difficulties in comparing CT enterography and video capsule endoscopy. *Eur Radiol* 2012; **22**: 1167-1171 [PMID: 22447355 DOI: 10.1007/s00330-012-2398-1]
- 39 **Scarsbrook AF**, Ganeshan A, Statham J, Thakker RV, Weaver A, Talbot D, Boardman P, Bradley KM, Gleeson FV, Phillips RR. Anatomic and functional imaging of metastatic carcinoid tumors. *Radiographics* 2007; **27**: 455-477 [PMID: 17374863 DOI: 10.1148/rg.272065058]
- 40 **Martínez-Sapiña Llanas MJ**, Ríos Reboredo A, Romay Cousido G, Romero González JA. Severe intestinal ischemia as a presenting feature of metastatic ileal carcinoid tumor: role of MDCT with coronal reformation in the early diagnosis. *Abdom Imaging* 2012; **37**: 558-560 [PMID: 22052449 DOI: 10.1007/s00261-011-9815-9]
- 41 **Pantongrag-Brown L**, Buetow PC, Carr NJ, Lichtenstein JE, Buck JL. Calcification and fibrosis in mesenteric carcinoid tumor: CT findings and pathologic correlation. *AJR Am J Roentgenol* 1995; **164**: 387-391 [PMID: 7839976 DOI: 10.2214/ajr.164.2.7839976]
- 42 **Hristova L**, Placé V, Nemeth J, Boudiaf M, Laurent V, Soyer P. Small bowel tumors: spectrum of findings on 64-section CT enteroclysis with pathologic correlation. *Clin Imaging* 2012; **36**: 104-112 [PMID: 22370131 DOI: 10.1016/j.clinimag.2011.08.011]
- 43 **Pelage JP**, Soyer P, Boudiaf M, Brocheriou-Spelle I, Dufresne AC, Coumbaras J, Rymer R. Carcinoid tumors of the abdomen: CT features. *Abdom Imaging* 1999; **24**: 240-245 [PMID: 10227886]
- 44 **Hoeffel C**, Crema MD, Belkacem A, Azizi L, Lewin M, Arrivé L, Tubiana JM. Multi-detector row CT: spectrum of diseases involving the ileocecal area. *Radiographics* ; **26**: 1373-1390 [PMID: 16973770 DOI: 10.1148/rg.265045191]
- 45 **Sheth S**, Horton KM, Garland MR, Fishman EK. Mesenteric neoplasms: CT appearances of primary and secondary tumors and differential diagnosis. *Radiographics* 2006; **23**: 457-473; quiz 535-536 [PMID: 12640160 DOI: 10.1148/rg.232025081]
- 46 **Horton KM**, Kamel I, Hofmann L, Fishman EK. Carcinoid tumors of the small bowel: a multitechnique imaging approach. *AJR Am J*

Roentgenol 2004; **182**: 559-567 [PMID: 14975946 DOI: 10.2214/ajr.182.3.1820559]

47 **Soyer P**, Dohan A, Eveno C, Dray X, Hamzi L, Hoeffel C, Kaci R,

Boudiaf M. Carcinoid tumors of the small-bowel: evaluation with 64-section CT-enteroclysis. *Eur J Radiol* 2013; **82**: 943-950 [PMID: 23480964 DOI: 10.1016/j.ejrad.2013.02.013]

P- Reviewer: Faintuch S, Juergens KU, Srivastava M

S- Editor: Tian YL **L- Editor:** A **E- Editor:** Wu HL





Published by **Baishideng Publishing Group Inc**

8226 Regency Drive, Pleasanton, CA 94588, USA

Telephone: +1-925-223-8242

Fax: +1-925-223-8243

E-mail: bpgoffice@wjgnet.com

Help Desk: <http://www.wjgnet.com/esps/helpdesk.aspx>

<http://www.wjgnet.com>

